Journal of Forensic Science & Criminology
Volume 7 | Issue 1
ISSN: 2348-9804

Research Article Open Access

A Preliminary Evaluation Study to Determine the Effectiveness of Infra-Red Photography for the Rapid Visualisation of Gun Shot Residue on Fabric

Rhodes C*, Beavan E and Smith P

University of Portsmouth, Institute of Criminal Justice Studies, Hampshire, UK

***Corresponding author:** Rhodes C, University of Portsmouth, Institute of Criminal Justice Studies, Ravelin House, Museum Road, Portsmouth, Hampshire PO12QQ, UK, E-mail: Claire.rhodes@port.ac.uk

Citation: Rhodes C, Beavan E, Smith P (2019) A Preliminary Evaluation Study to Determine the Effectiveness of Infra-Red Photography for the Rapid Visualisation of Gun Shot Residue on Fabric. J Forensic Sci Criminol 7(1): 103

Received Date: April 1, 2018 **Accepted Date:** April 22, 2019 **Published Date:** April 24, 2019

Abstract

Infrared (IR) photography has been shown to be a proficient technique for the examination of documents, blood traces and ageing of skin injuries. However, its application in relation to the visualisation of latent Gunshot Residue (GSR) deposits has, until now, been significantly under researched. This paper evaluates the effectiveness of IR photography as a rapid technique for GSR visualisation on different fabric types.

The Attestor Forensics Scene View BV800 viewing system was used to visualise GSR deposits, produced by a Glock 17 9x19mm and 9mm Luger ammunition, on four different fabric types and at three firing distances of 50mm, 200mm and 1000mm. The results demonstrate that IR photography can produce comparable results to other GSR visualisation techniques, without the limitations of disturbing the sample's structure or being obstructed by certain material types.

Keywords: Crime Scene; Distance Determination; Firearms; Gunshot Residue Visualisation; Infra-Red Photography; Clothing

List of abbreviations: ALS: Alternative Light Sources; FSR: Forensic Science Regulator; GSR: Gun Shot Residue; HMIC: Her Majesty's Inspectorate of Constabulary; IR: Infra-red; MGT: Modified Greiss Test; SEM: Scanning Electron Microscope; SPSS: Statistical Package for the Social Sciences; UK: United Kingdom; XRF: X-ray Flourescence

Introduction

Firearm related incidents in England and Wales constitutes 0.2% of all police recorded crime. Of those cases, 56% involved a firearm discharge [1]. Despite this seemingly small number of crimes, the community and societal impact of gun crime are considerable, leading to the intensification of violent behaviour, robbery, drug dealing and prostitution, posing a major risk to public safety [2-4].

During the investigation of firearms incidents Gunshot Residue (GSR) is often the only evidence providing a link between the scene, the shooter and the firearm itself [5]. In general, Forensic Ballistics remains one of the most underdeveloped and under researched areas of forensic practice, with the complex and dynamic nature of GSR formation being frequently contested [6,7]. In the United Kingdom (UK) both Her Majesty's Inspectorate of Constabulary (HMIC) (2013) and the Forensic Science Regulator (FSR) (2015) believe that the standard of forensic procedures relating to firearms evidence, is not meeting regulatory requirements [8,9]. The regulator concluded that, these sub-standard practices were due to insufficient knowledge and inconsistent levels of expertise among staff, combined with the use of unaccredited processes and techniques [9]. This is unsurprising, given that the regulatory standards for the firearms evidence procedures are in their preliminary stages [10].

Despite the complex mechanics of GSR formation and deposition, it frequently presents repeatable features, which are characteristic of variable changes, such as distance or ammunition type [11-13]. However, many academics have criticised the evidential value of such determinations, on the basis that insufficient data exists regarding the true extent of the influence that variables, such as rate of deposition, transferal and persistence have upon GSR deposits. They argue that this makes it difficult to determine the probative value of such evidence and subsequently impedes its judicial worth [14-16].

Researchers have endeavoured to use Bayesian networks to overcome the complexities of GSR analysis imposed by the vast number of conflicting variables and concluded that, despite Bayesian systems providing a structure for the systematic analysis of the combined influence that multiple variables have upon GSR formation, its output is dependent upon the validity of the research conducted at each variable level [14,15]. Taking these factors into account it is clear that further research must be undertaken into cost-effective forensic techniques, which are efficient, whilst advancing their forensic ballistics capabilities and enhancing the analysis and subsequent evidential value of GSR evidence.

A key limitation of GSR analysis is that few visualisation techniques can be conducted at the crime scene [17]. This is a major disadvantage as packaging and transportation of samples often causes damage to fragile GSR deposits, reducing the probative and evidential value [18-21]. Alternative Light Sources (ALS) have been utilised as a quick and non-destructive method to enhance the visualisation of GSR for distance determination on clothing, using an optimum wavelength range of 440-580nm [22]. ALS has been shown to provide poor results for fabrics with tight weaves and dark colours or backgrounds as they fluoresce, obscuring the GSR deposit [6,22,23].

Digital Infrared (IR) photography could address these issues; as its portability allows it to be easily transported to scenes for in-situ examinations and its unobtrusive nature leaves the deposits' physical structures undisturbed, thus demonstrating advantages over other techniques, such as chemical tests [7,24]. Despite these obvious advantages, little research has been undertaken on IR photography's proficiency as a GSR visualisation technique [25].

IR photography allows visualisation of otherwise invisible GSR on multiple types of clothing, varying in colour and fibre typology, with rayon producing the best results [24,26]. It is also capable of visualising GSR deposits that would otherwise be obscured by bloodstained or patterned materials [27]. Although accurate, previous research is limited, given that it only uses three different material types and the effect of increasing distance was not examined.

This research will examine the effectiveness of digital IR photography for the visualisation of GSR using a multidimensional approach which evaluates the influences of both increasing distance and material type.

Materials and Methods

Firing was carried out within a 50m indoor police shooting range, the air was still and the air-conditioning was turned off [28]. All shots were fired by a police firearms specialist. The angle of firing was maintained at ninety degrees to the target [29]. The Glock 17, 9x19mm handgun was selected for this study, as handguns are regularly observed within UK gun crimes. The type of ammunition utilized was 9mm Luger 124 GRAIN HST tactical law enforcement ammunition and was selected based on its availability.

To effectively evaluate the relationship between each fibre's differing chemical and structural properties and visualisation of GSR, two of the most common fibre types were taken from each of the two main classifications; natural and man-made [30]. From the natural classification, wool and cotton were selected; for the man-made classification, viscose and polyester were selected; with each item of clothing in varying shades of the same blue colour, comprising 100% of the desired fibre source. Six 250mm square sections were cut from each of the four garments and stapled to a shooting target. Three distances were selected, 50mm, 200mm and 1000mm [12,31-33]. Two samples of each material were shot through at each distance, producing twenty-four samples in total.

Post shooting, the target samples were packaged individually into paper evidence bags, compliant with forensic regulations [34]. No two target samples were placed within the same bag and each bag was labelled with the date, time, firing distance and material type. The samples were then transported back to the laboratory for analysis.

Analysis of the GSR deposits was first undertaken with standard visible light. A 35 mm Nikon D-70 camera fitted with a Nikon Nikkor AF 70-300mm f/4-5.6 G lens was utilised to photograph the GSR deposits within the visible light spectrum. The camera was mounted on a copy stand, with the camera-to-sample distance varying between 20cm to 40cm.

For the examination of the samples under IR photography the Attestor Forensics Scene View BV800 viewing system was utilised. This system was able to visualise light at wavelengths of 850nm, thus falling within the IR spectrum [26]. Before any GSR sample photographs were taken, IR photographs were taken of the remaining segments of the fabrics which had not been shot, acting as a control to evaluate any background fluorescence which may be mistaken for GSR deposits.

To analyse the effectiveness of IR photography, comparisons were made regarding four features of the GSR deposits against standard visual examination. Four data-sets were originally recorded regarding the dimensions of the GSR originating from the bullet hole (left, right, up and down), a method adapted from Gerard *et al.* [35]. However, due to the complexity of analysing these four data-sets under both IR and visual examinations, they were combined to produce the GSR lateral and vertical diameters. The approximate number of the larger independent residue particles was recorded, referring to the larger independent solid formed fragments, opposed to the much smaller collective smoke particles, which constitute the vaporous soot residue [35-37]. Given limitations regarding available technology to accurately measure the residual density, a reference scale was created, based upon the observations of Tugcu *et al.*, Brozek-Mucha and Haag & Haag [38-40] (Table 1).

Scale Number	Description of Residue
0	No visible smoke/soot residue, only bullet wipe visible
1	Little or no visible smoke/soot residue, only a wide scattering of larger particles.
2	Smoke/soot residue is present, however only forming a partially grey clouding and its visibility is variable. Large particles are present and numerous.
3	Very thick and dense particle or smoke/soot residue deposited around the bullet hole, often accompanied by burn-marks. This forms a black/grey mass that gradually weakens with distance. Few larger particles present.

Table 1: Reference scale corresponding to the residue density

Statistical analysis, including a one-way between-groups analysis of variance, were conducted using a Statistical Package for the Social Sciences (SPSS) to determine the impact that the distance of firing and the target material had upon the formation and constituency of GSR deposits.

Results

Under basic visual examination (utilising the visible light camera), GSR could only be identified on three of the four materials at the 50mm firing distance, with polyester displaying no visible GSR. At 200mm minor traces of GSR were visible on one viscose and one cotton target. At 1000mm no GSR was visualised on any material. Using IR visualisation GSR deposits were identified on all target materials at all distances, with the exception of one viscose target at 1000mm.

Under visual analysis the mean vertical and lateral diameters of GSR deposits at 50mm on all materials were 52.8mm and 62.4mm respectively. Under IR photography the mean vertical and lateral diameters were larger at 75.5mm and 70.4mm respectively. At 200mm the mean vertical and lateral diameters under visual analysis demonstrate reductions to 8.8mm and 11.3mm respectively, however under IR analysis they are seen to increase 105.5mm and 108mm (Figures 1,2 and 3).

Under IR examination, the lateral diameters on 96% of the targets across all distances were on average 149mm wider; vertical diameters on 88% of targets across all distances showed an average increase of 470mm in dispersal.

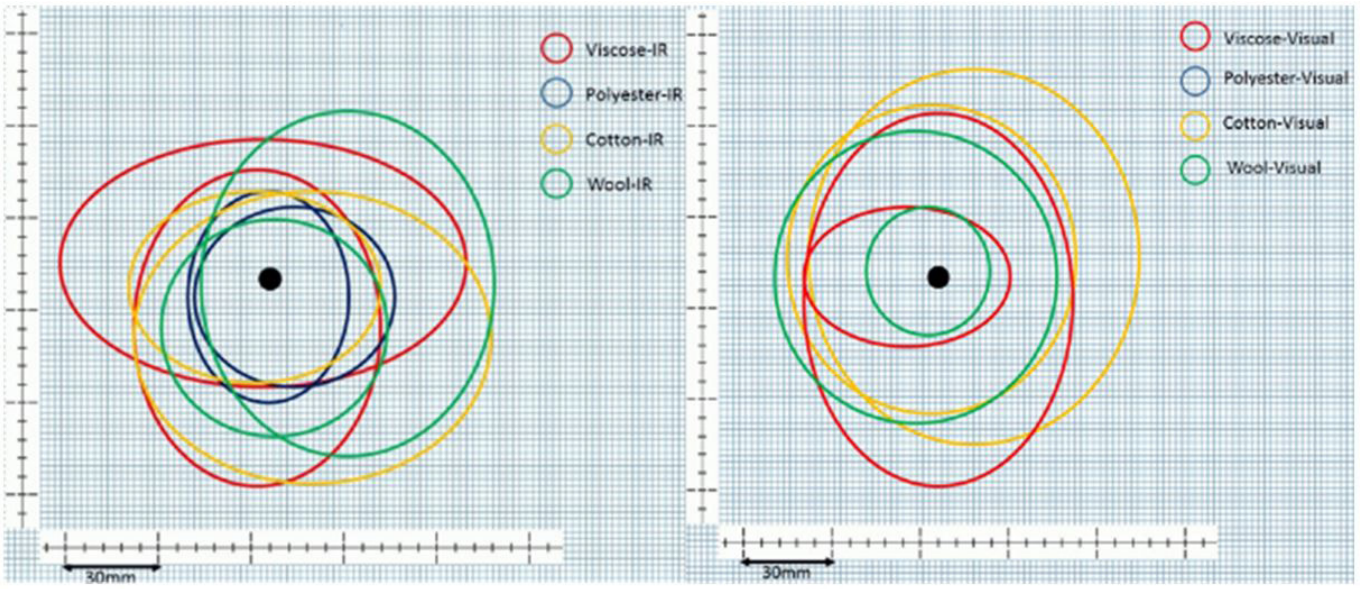

Figure 1: Comparison of the GSR deposits spatial distribution at the 50mm firing distance, under IR examination (Left) and visual examination (right). The occurrence of two rings with the same colour represents the two shot that were taken for each material type, the absence of a particular colour ring demonstrates that no GSR was identified

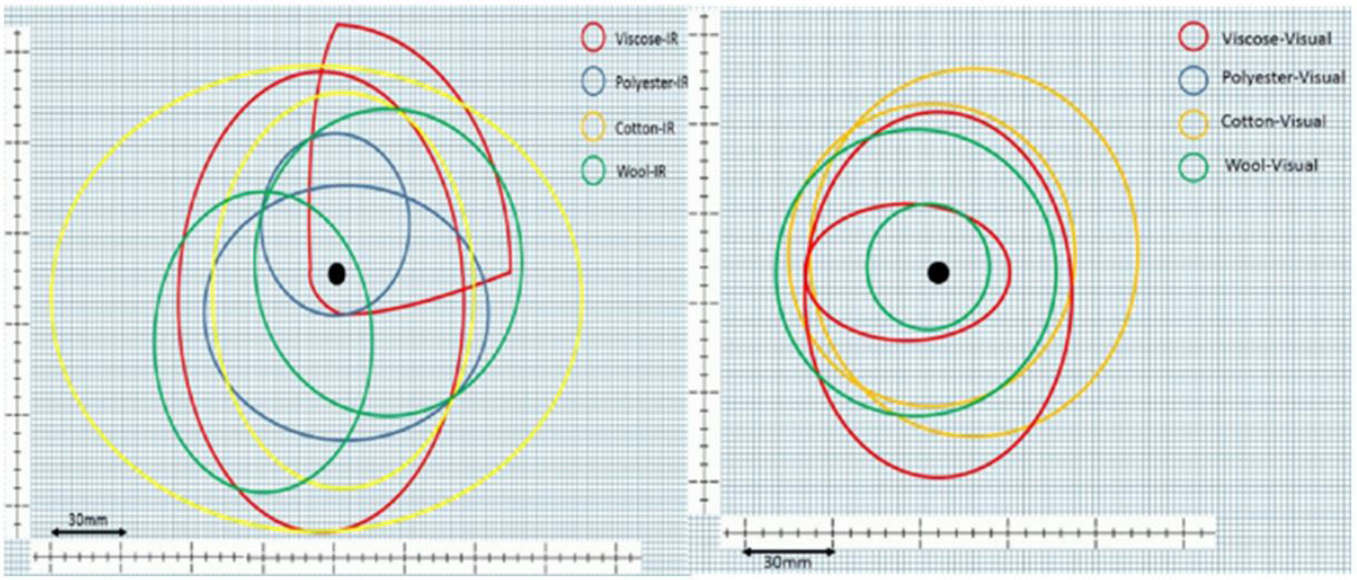

Figure 2: Comparison of the GSR deposits spatial distribution at the 200mm firing distance, under IR examination (left) and visual examination (right)

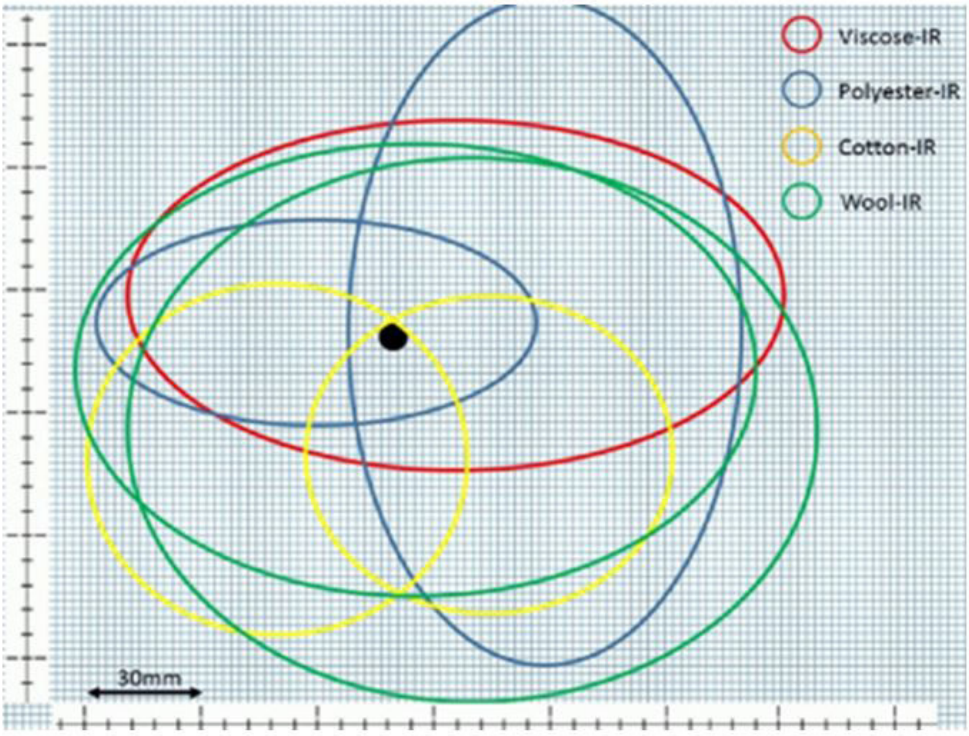

Figure 3: The GSR deposits spatial distribution at the 1000mm firing distance under IR examination. No residue was visible under visual

The average residue densities of the GSR deposits increased under IR analysis at all distances (Figure 4). The residue density and frequency of the larger independent particles, identified upon the polyester targets, were less than the other material types; with viscose producing the most. Only the results produced under IR examination were used for the statistical analysis of the effects increasing distance and differing target material had upon the formation of the GSR.

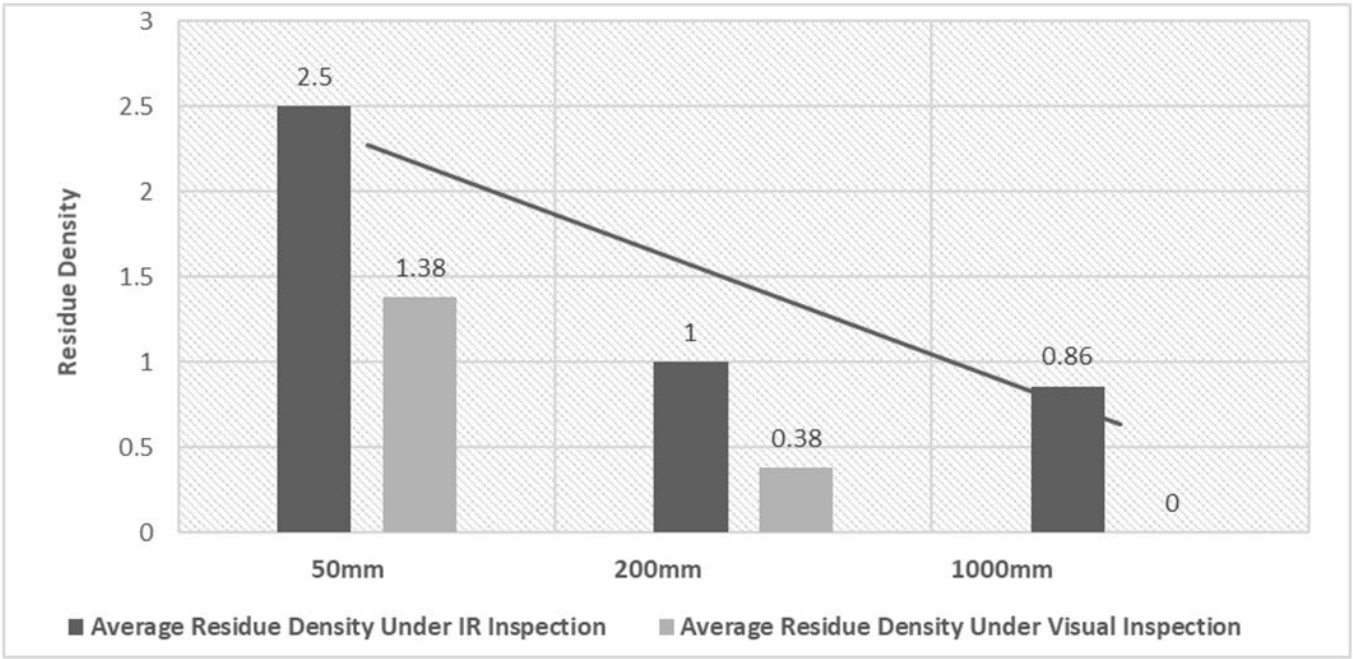

Figure 4: Comparison of the average residue densities under IR and visual examinations

A one-way between-groups analysis of variance was conducted to determine the impact that the target clothing material had upon the formation and constituency of GSR deposits when visualised using IR photography. By establishing the four material types as independent variables, significant differences could be identified within the recorded scores of the four features of GSR.

There was no statistically significant difference within the four recorded features of GSR deposits at the $p < .05$ level across the different categories of material. GSR lateral diameter: $F(3, 23) = .119$, $p = .948$; GSR vertical diameter: $F(3, 23) = .563$, $p = .646$; the approximate number of the larger independent particles: $F(3, 23) = .424$, $p = .738$; Residue density: $F(3, 23) = .197$, $p = .897$.

Overall GSR adhered less frequently to the polyester targets, with the GSR lateral diameters an average of 940mm smaller, than those identified upon the other targets, and the vertical diameters being an average of 239mm smaller. Conversely, the other man-made target material, viscose, showed the greatest propensity for retention of GSR deposits. The GSR lateral diameters identified upon the viscose targets were on average 170mm larger than those identified on the other targets and their vertical diameters were an average of 745mm larger.

A one-way between-groups analysis of variance was conducted to determine the impact that the distance of firing had upon the formation and constituency of GSR deposits when visualised using IR Photography. Measurements were based upon four features of the GSR deposits, the residue diameters laterally and vertically, the residue density and the approximate number of the larger independent particles. There were no statistically significant differences at the $p < .05$ level for the recordings of the residue's diameters laterally or vertically. GSR lateral diameter: $F (2, 23) = 1.739$, $p = .2$; GSR vertical diameter: $F (2, 23) = 2.054$, $p = .153$; the approximate number of the larger independent particles: $F (3, 23) = .424$, $p = .738$; Residue density: $F (3, 23) = .197$, $p = .897$.

The frequency of the larger independent particles revealed statistical significance at the $p < .05$ level for the three distances: $F (2, 23) = 9.4$, $p = .001$. The effectual size, calculated using eta squared, was .47. Post-hoc analysis using the Bonferroni test demonstrated that the number of these larger particles at 50mm (M=77.75, SD=55.35) was statistically different than at 200mm (M=171.38, SD=68.43) and 200mm itself statistically different from 1000mm (M=60.5, SD=36.71). However, the 1000mm group was not statistically different from the 50mm group.

Upon the 200mm targets a residual ring could be observed, outside of the central residue pattern (Figure 5).

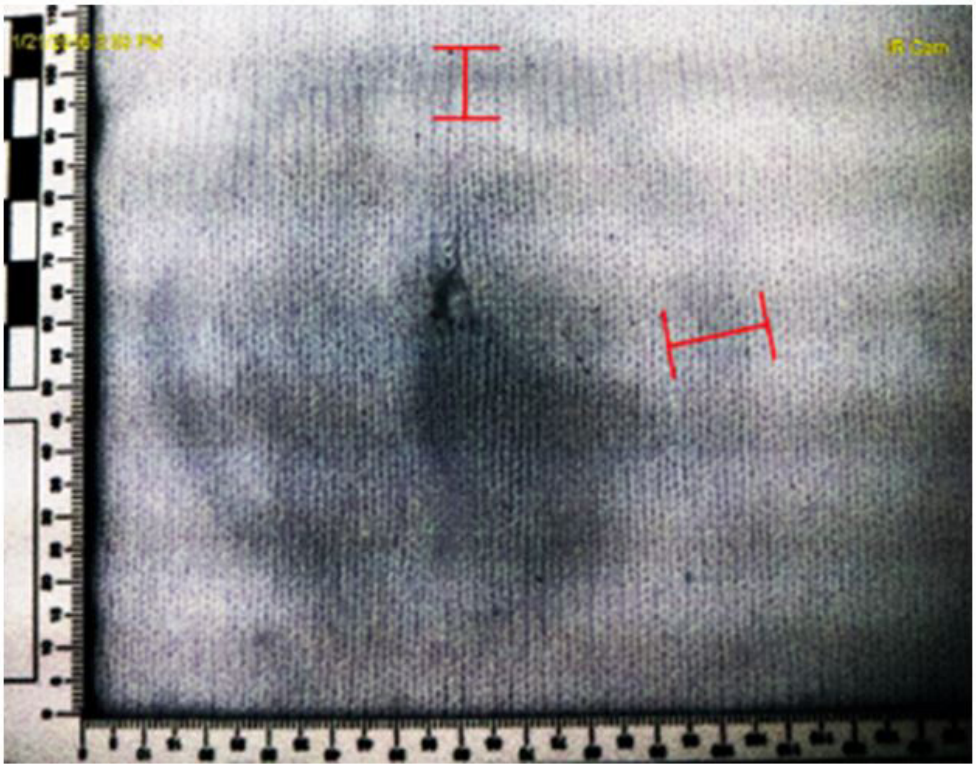

Figure 5: Example of residual ring observed on cotton target at 200mm

Discussion

Visual analysis of GSR distributions is augmented under IR examination, significantly enhancing the visualization of GSR upon all target materials. The results correlate strongly with other studies which have utilised chemical treatments, alternative light sources and x-ray fluorescence [6,22,24,41-44].

The fact that GSR was identified upon the 1000mm target is significant, given that other techniques, such as X-ray Fluorescence (XRF) and ALS, have been limited to identifying GSR from firing distances under 600 mm [22,44,45]. Comparison between the results for the GSR lateral diameters and those produced by Bailey, Casanova and Bufkin, suggest that IR photography is superior at visualising GSR compared to the Modified Greiss Test (MGT) [46].

However, this comparison is limited; as even though the distribution of GSR particles has been shown to be similar across pistols it is highly dependent on the ammunition used [47]. Differing ammunition types have been shown to cause significant variance within GSR deposits, thus reducing the validity of cross-study comparisons and the extrapolation of results to other handguns and ammunition [28,48].

The results also suggest that differences within target material fibre typology will not impact the formation or consistency of GSR deposits, opposing what is suggested within the literature [6,39]. A potential explanation for these conflicting results is that the detection of GSR is not dependent upon the fibre morphology of the material, but rather upon its colour and weave rigidity, with darker backgrounds offering the least visible deposits; explaining the variance observed across the four material types [22,31].

Despite previous research suggesting that natural fibres, such as cotton or wool, demonstrate the greatest adherence of frequencies, it is therefore surprising that in this study man-made viscose fibres showed the highest propensity for adherence [31,39,49]. However, a previous study that utilised IR photography concluded that rayon fabrics displayed the highest frequencies of GSR particles [24]. Rayon and viscose fibres adopt very similar structures and are manufactured from cellulose molecules containing identical hydroxyl groups meaning that these results demonstrate that IR photography is particularly good at enhancing the visualisation of GSR upon manmade cellulolytic fibres [50]. These findings suggest that the characteristics of materials will inhibit some visualisation techniques more than others, with IR photography being most efficient on darker man-made fabric compared to XRF and ALS [6,24,27,44].

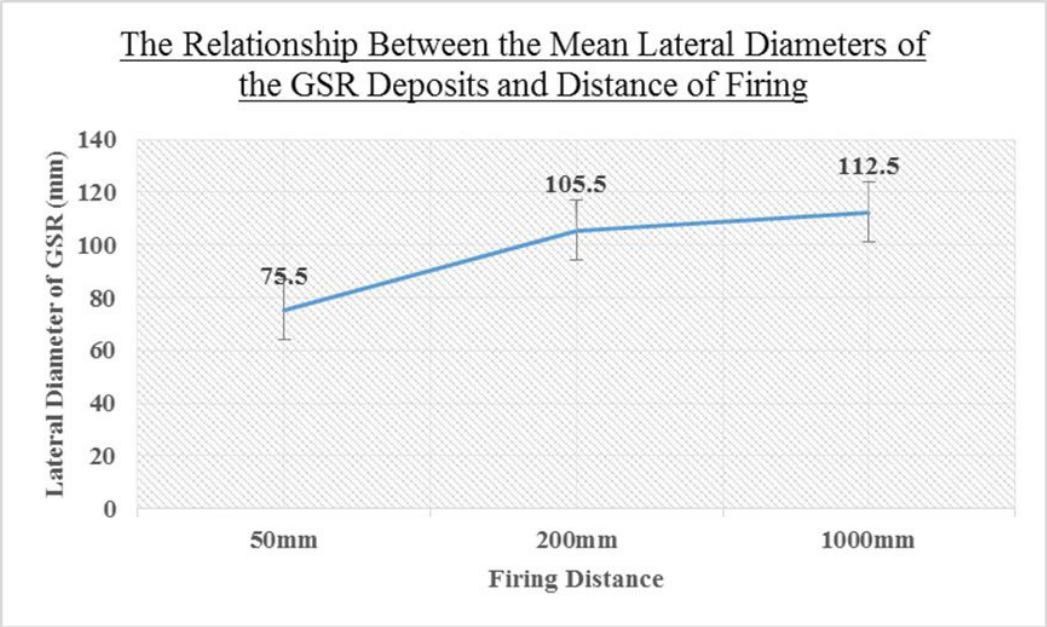

Figure 6: The relationship between the mean lateral diameters of the GSR deposits and the distance of firing

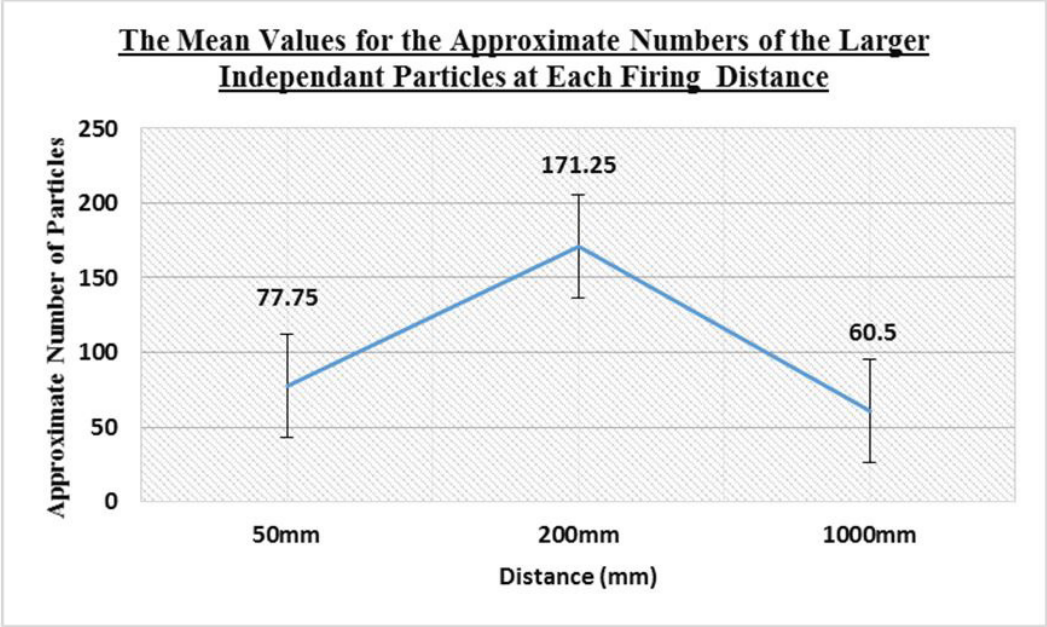

Figure 7: The relationship between the approximate numbers of the larger independent particles and increasing firing distance

There is an increasing association between the firing distance and the GSR lateral diameters, this is unsurprising given that such a correlation is prominent within the literature [40,41,51] (Figure 6). The reason that this correlation did not reach statistical

significance, is likely due to the low number of independent variables (distances) tested, thus not permitting the mean difference to reach significance. Alongside distance the frequency of the larger particles increases, until an unknown point between 200mm and 1000mm is reached, in which this frequency starts decreasing (Figure 7).

This increasing positive correlation between the firing distance and the frequency of GSR particles, displayed by the 50mm and 200mm distances, was not unsurprising, given the literature's indication of such a result [39,52]. Additionally, referring back to the conflicting results regarding the relationship between the larger GSR partial frequencies and increasing range, these results appear to support Dillon and Brozek-Mucha [53,54].

The oscillation displayed by the rising and falling of the frequency of the larger GSR particles across increasing firing distances, has been similarly observed by Brozek-Mucha and Santos *et al.*, for the constituent particles Sb and Br. Therefore, referring back to the concepts proposed by Chang *et al.* and Turillazzia *et al.*, it is likely that at firing distances of 200mm, the amplified energies of these larger particles is at equilibrium with the resistance force of the atmosphere [5,13,39,55]. So as the distance advances beyond this point, the resistance force will increase, thus gaining dominance, meaning that increasingly fewer particles will reach the target. Therefore, indicating that Bhattacharyya's theoretical model is only applicable to firing distances under approximately 200mm [56].

The residual ring outside the central residue pattern on the 200mm targets is an unexpected observation, as the literature describes a simple linear decrease in GSR residue intensification away from the bullet hole [35-37]. This pattern does reflect previous findings which show that these rings are consistent with heavy metal/lead free ammunition, due to the higher quantities of Gadolinium (Gd) [44]. However, this type of ammunition was not used during this experiment. The identification of this gadolinium residue pattern, raises questions regarding IR photography's potential to identify GSR originating from lead or heavy metal free ammunition. XRF and SEM analysis have previously been utilised to visualise GSR originating from such ammunitions [43,57,58]. The identification of this pattern typology strengthens IR photography's validity as a GSR visualisation technique by demonstrating its ability to detect differing forms of constituent GSR particles.

Conclusion

The aim of this research was to evaluate the effectiveness of IR photography as a rapid and efficient technique for GSR visualisation and the results indicate that IR photography significantly enhances the visualization of GSR upon all target materials. From a practical perspective the unobtrusiveness of IR photography clearly demonstrates a significant advantage over the often destructive nature of chemical tests [6].

From a practical standpoint, IR photography's capacity to visualise GSR deposits upon target materials, irrespective of the fabric morphology, is of significant importance given that it strengthens the evidential value of distance determinations, by reducing variable level inconsistencies, which has informed previous criticisms regarding the evidential value of determinations derived from GSR analysis [14,15,59]. Moreover, this demonstrates another advantage of IR photography over XRF and ALS, given that their effectiveness can be diminished by particular colours or thicknesses.

Overall, given that such correlations regarding GSR formation were identified, demonstrates IR photography's propensity to provide an early assessment tool for samples suspected of containing GSR deposits. A crucial advantage, as only the most beneficial samples will be referred for more advanced and costly examinations [60]. Despite IR photography producing comparable results to other techniques, such as XRF, ALS and chemical tests, its portable and non-destructive nature offers greater practicality than these methods; making IR photography a suitable technique when considering budgetary and capability limitations [45,51,60].

References

1. Office for National Statistics (2015) Crime Statistics, Focus on Violent Crime and Sexual Offences, 2013/14 Release: Chapter 3: Violent Crime and Sexual, London.

2. Lupton R, Wilson A, May T, Warburton H, Turnbull PJ (2002) A rock and a hard place: drug markets in deprived neighbourhoods. Home Office Research Study 240, London: Home Office.

3. Pearson, Geoffrey, Hobbs, Richard, Jonesetr, et al. (2001) Middle market drug distribution. Home Office Research Study 227. London: Home Office.

4. Wilson A, May T, Warburton H, Lupton R, Turnbull PJ (2002) Heroin and Crack Cocaine Markets in Deprived Areas: Seven Local Case Studies. Supplement to Home Office Research Study 240: 'A Rock and a Hard Place: Drug Markets in Deprived Neighbourhoods'. CASE Report 19. London: Centre for Analysis of Social Exclusion, UK.`

5. Chang KH, Jayaprakash PT, Yew CH, Abdullah AF (2013) Gunshot residue analysis and its evidential values: a review. Aust J Forensic Sci 45: 3-23.

6. Kersh KL, Childers J, Justice D, Karim G (2014) Detection of Gunshot Residue on Dark-Coloured Clothing Prior to Chemical Analysis. J Forensic Sci 59: 754-62.

7. Dalby O, Butler D, Birkett JW (2010) Analysis of gunshot residue and associated materials – a review. J Forensic Sci 55: 924-43.

8. JusticeInspectorates (2013) Making the Connections: A thematic inspection of police force compliance with the Memorandum of Understanding between the National Ballistics Intelligence Service and Police Forces. London: Her Majesty's Inspectorate of Constabulary, UK.

9. Tully G (2015) Forensic Science Regulator Annual Report: November 2014 – November 2015. London: Forensic Science Regulator.

10. Bolton-King RS (2016) Preventing miscarriages of justice: A review of forensic firearm identification. Sci Justice 56: 129-4

11. Brozek-Mucha Z (2007) Comparison of cartridge case and airborne GSR – a study of the elemental composition and morphology by means of SEM-EDX, X-ray Spectrum. J Forensic Sci 36: 398-407.

12. Mou Y, Lakadwar J, Rabalais JW (2008) Evaluation of Shooting Distance by AFM and FTIR/ATR Analysis of GSR. J Forensic Sci 53: 1381-6.

13. Turillazzia E, Peria GP, Nieddub A, Belloa S, Monacic F, et al. (2013) Analytical and quantitative concentration of gunshot residues (Pb, Sb, Ba) to estimate entrance hole and shooting-distance using confocal laser microscopy and inductively coupled plasma atomic emission spectrometer analysis: An experimental study. Forensic Sci Int 231: 142-9.

14. Biedermann A, Bozzab S, Taronia T (2009) Probabilistic evidential assessment of gunshot residue particle evidence (Part I): Likelihood ratio calculation and case pre-assessment using Bayesian networks. Forensic Sci Int 191: 24-35.

15. Biedermann A, Bozzab S, Taronia T (2009) Probabilistic evidential assessment of gunshot residue particle evidence (Part II): Bayesian parameter estimation for experimental count data. Foren Sci Int 191: 24-35.

16. Romolo SR, Margot P (2001) Identification of Gunshot Residue: A Critical Review. Forensic Sci Int 119: 195-211.

17. Duarte A, Silva LM, Souza CT, Stori EM, Boufleur LA, et al. (2015) Elemental quantification of large gunshot residues. Proceedings of the 14th International Conference on Nuclear Microprobe Technology & Applications.

18. Benito S, Abrego Z, Sánchez A, Unceta N, Goicolea MA, et al. (2014) Characterization of organic gunshot residues in lead-free ammunition using a new sample collection device for liquid chromatography–quadrupole time-of-flight mass spectrometry. Forensic Sci Int 246: 79-85

19. Gilchris E, Jongekrijg F, Harvey L, Smit N, Barron L (2012) Characterisation of gunshot residue from three ammunition types using suppressed anion exchange chromatography. Forensic Sci Int 221: 50-6.

20. Wallace JS (2008) Chemical Analysis of Firearms, Ammunition and Gunshot Residue. Florida: CRC Press.

21. Zeichner A, Eldar B (2004) A novel method for extraction and analysis of gunpowder residue on double-side adhesive coated stubs. J Forensic Sci, 49: 1194-206.

22. Atwater CS, Durina ME, Durina JP, Blackledge RD (2006) Visualization of Gunshot Residue Patterns on Dark Clothing. J Forensic Sci 51: 1091-5.

23. Charles S, Lannoy M, Geusens N (2013) Influence of the type of fabric on the collection efficiency of gunshot residues. Forensic Sci Int 228: 42-46.

24. Bailey JA (2007) Digital infrared photography to develop GSR. Aust J Forensic Sci 39: 33-40

25. Lin AC, Hsieh HM, Tsai LC, Linacre A, Lee JC (2007) Forensic Applications of Infrared Imaging for the Detection and Recording of Latent Evidence. J Forensic Sci 52: 1148-50.

26. Trostle F (1988) Photographic examination of gunshot powder burn patterns through the use of infrared film. J Forensic Identif 38: 57-61.

27. De Broux ST, McCaul KK, Shimamoto S (2007) Infrared Photography. Crime Scene Investigator 1-22.

28. Malevski H, Judokaitė-Granskienė G (2009) Gun smoke distribution from various firearms In: Criminalistics and Forensic Examination: Science, Studies, Practice, Lietuvos teismo ekspertizės centras: Vilnus, Lithuania.

29. Gray DE (2004) Doing Research in the Real World. London: SAGE Publications Ltd., USA.

30. Robertson JR (1999) Classification of Textile Fibres: Production, Structure, and Properties In: Forensic Examination of Fibres (2nd Edn) London: CRC Press, UK.

31. Ananth V, Ahmad UK, Tong SM (2011) Detection of Organic Gunshot Residues for the Estimation of Firing Distance. Malay J Forensic Sci 2: 36-45.

32. Glattstein B, Vinokurov N, Zeichner A (2000) Improved method for shooting distance estimation. Part 1, bullet holes in clothing items. J Forensic Sci 45: 801-6.

33. Krishnan SS (1967) Firing distance determination by neutron activation analysis. J Forensic Sci 12: 471-83.

34. Forensic Science Regulator (2011) Codes of Practice and Conduct for forensic science providers and practitioners in the Criminal Justice System. London: Forensic Science Regulator.

35. Gerard RV, McVicar MJ, Lindsay E, Randall ED, Harvey E (2011) The long range deposition of gunshot residue and the Mechanism of Its Transportation. Can Forensic Sci J 44: 97-104.

36. Fojtášek L, Vacinová J, Kolář P, Kortlý M (2003) Distribution of GSR particles in the surroundings of shooting pistol. Forensic Sci Int 132: 99-105.

37. Zeichner A, Glattstein B (2002) Recent Developments in the Methods of Estimating Shooting Distance. The Sci World J 2: 573-85.

38. Tugcu H, Yorulmaz C, Bayraktaroglu G, Bulent Uner H, Karslioglu Y, et al. (2005) Determination of Gunshot Residues with Image Analysis: An Experimental Study. Mil Med 170: 802-5.

39. Brozek-Mucha Z (2011) Variation of the chemical contents and morphology of gunshot residue in the surroundings of the shooting pistol as a potential contribution to a shooting incidence reconstruction. Forensic Sci Int 210: 31-41.

40. Haag MG, Haag LC (2011) Shooting Incident Reconstruction. Oxford: Academic Press, UK.

41. Brown H, Cauchi DM, Holden JL, Wrobelb H, Cordnera S (1999) Image analysis of gunshot residue on entry wounds: I – The technique and preliminary study. Forensic Sci Int 100: 163-77

42. Brown H, Cauchi DM, Holden JL, Allen FC, Cordner S, et al. (1999) Image analysis of gunshot residue on entry wounds, II: a statistical estimation of firing range. Forensic Sci Int 100: 179-86.

43. Charpentier B, Desrochers, C (2000) Analysis of primer residue from lead free ammunition by x-ray micro-fluorescence. J Forensic Sci 45: 447-52.

44. Latzel S, Neimke D, Schumacher R, Barth M, Niewöhner L (2012) Shooting distance determination by m-XRF—Examples on spectra interpretation and range estimation. Forensic Sci Int 223: 273-8.

45. Flynn J, Stoilovic M, Lennard C, Prior I, Kobus H (1998) Evaluation of X-ray micro-fluorescence spectrometry for the elemental analysis of firearm discharge residues. Forensic Sci Int 97: 21-36.

46. Bailey JA, Casanova RS, Bufkin K (2006) A Method for Enhancing Gunshot Residue Patterns on Dark and Multi-coloured Fabrics Compared with the Modified Griess Test. J Forensic Sci 51: 812-4

47. Ditrich H (2012) Distribution of gunshot residues: The influence of weapon type. Forensic Sci Int 220: 85-90

48. Zeichner A, Levin N, Dvorachek M (1992) Gunshot residue particles formed by using ammunitions that have mercury fulminate based primers. J Forensic Sci 37: 1567-73.

49. Berk RE, Rochowicz SA, Wong M, Kopina MA (2007) Gunshot residue in Chicago police vehicles and facilities: an empirical study. J Forensic Sci 52: 838-41

50. Harry ID, Saha B, Cumming IW (2007) Surface properties of electrochemically oxidised viscose rayon based carbon fibres. Carbon 45: 66-74.

51. López-Lópeza M, García-Ruiz C (2014) Recent non-chemical approaches to estimate the shooting distance. Forensic Sci Int 239: 79-85.

52. Schwoeble AJ, Exline DL (2000) Current methods in forensic gunshot residue analysis. Boca Raton Florida: CRC Press, USA.

53. Dillon JH (1990) A protocol for gunshot examination in muzzle to target distance determination. Assoc Firearm and Tool Mark Examiners J 22: 257-74.

54. Brozek-Mucha Z (2009) Distribution and properties of gunshot residue originating from a Luger 9 mm ammunition in the vicinity of the shooting gun. Forensic Sci Int 183: 33-44.

55. Santos A, Ramos P, Fernandes L, Magalhães T, Almeida A, et al. (2015) Firing distance estimation based on the analysis of GSR distribution on the target surface using ICP-MS—An experimental study with a 7.65 mm × 17 mm Browning pistol (.32 ACP). Forensic Sci Int 247: 62-8.

56. Bhattacharyya CN (1989) Dispersion of firing discharge residues using a Maxwellian model. Forensic Sci Int 42: 271-7.

57. Martiny A, Campos AP, Sader MS, Pinto AL (2008) SEM/EDS analysis and characterization of gunshot residues from Brazilian lead-free ammunition. Forensic Sci Int 177: 9-17.

58. Polovková J, Šimonič M, Szegényi I (2015) Study of gunshot residues from Sintox® ammunition containing marking substances. Egypt J Forensic Sci 5: 174-9.

59. Biedermann A, Taronia F (2006) A probabilistic approach to the joint evaluation of firearm evidence and gunshot residues. Forensic Science International 163: 18-33.

60. Richardson D (2014) Oral Evidence Taken before the Science and Technology Committee. House of Commons: Science and Technology Committee, London.